Check for updates

ASME Journal of Engineering for Gas Turbines and Power
Online journal at:
https://asmedigitalcollection.asme.org/gasturbinespower

Experimental Results of a Novel Two-Phase Water Ejector Design for High-Temperature Heat Pump Applications

Omar Abu Khass[1]
Institute of Low-Carbon Industrial Processes,
German Aerospace Center,
Cottbus/Zittau 03050/02763, Germany
e-mail: omar.abukhass@dlr.de

Marco Cristofaro
Institute of Software Methods for
Product Virtualization,
German Aerospace Center,
Dresden 01187, Germany

Steffen Klöppel
Institute of Low-Carbon Industrial Processes,
German Aerospace Center,
Cottbus/Zittau 03050/02763, Germany

Eberhard Nicke
Institute of Low-Carbon Industrial Processes,
German Aerospace Center,
Cottbus/Zittau 03050/02763, Germany

Panagiotis Stathopoulos
Institute of Low-Carbon Industrial Processes,
German Aerospace Center,
Cottbus/Zittau 03050/02763, Germany

High-temperature heat pumps (HTHPs) are a key technology for decarbonizing industrial process heat. Within such systems, two-phase water ejectors offer a promising opportunity to function as secondary steam compressors. By entraining hot steam with high-pressure water, they enable simultaneous cooling and pressure increase, thereby reducing both the power consumption and the number of mechanical compressor stages required. This integration has the potential to significantly enhance the energy efficiency and economic viability of HTHPs. However, the internal flow dynamics of two-phase ejectors remain insufficiently understood, particularly under the demanding high-pressure and high-temperature operating conditions relevant for heat pump applications. In the mixing region of the ejector, where the two-phase flow approaches critical design conditions, the speed of sound is strongly affected, potentially giving rise to shock structures and strong variations in thermophysical properties. The lack of experimental insights into these phenomena limits the reliable design and optimization of ejectors for industrial applications. This paper investigates how two-phase water ejectors can be experimentally characterized to advance their efficient integration into HTHP systems. To address this, a novel closed-loop experimental facility has been developed, enabling continuous operation with a flexible operating range of water and steam conditions representative of different potential heat pump architectures. The facility integrates novel designs for the nozzle and mixing chamber, a water separation and condensation system, and advanced sensors and control strategies to precisely regulate inlet and outlet conditions. The ejector has been designed based on prior CFD simulations by the authors, allowing comparison of numerical and experimental results. Preliminary tests provide performance indicators such as pressure ratio and entrainment ratio. This work delivers new ejector components designs, with a custom experimental methodology and initial results that deepen the fundamental understanding of two-phase ejector behavior. It thereby contributes to the optimized application of ejectors as efficient compression components in next-generation high-temperature heat pump systems.
[DOI: 10.1115/1.4072528]

Keywords: two-phase ejector, high-temperature heat pump, experimental facility design, steam compression

1 Introduction

The decarbonization of industrial process heat represents one of the key challenges in the transition toward sustainable and carbon-neutral production. In this context, high-temperature heat pumps (HTHPs) have gained increasing attention as a promising solution for providing steam in temperature ranges above 120 °C. By utilizing electricity, HTHPs can recover and upgrade low-grade waste heat, thereby significantly reducing primary energy consumption and greenhouse gas emissions [1]. Among the potential working fluids, water is particularly attractive due to its high latent heat of vaporization, environmental neutrality, and high critical temperature of 374 °C [2]. However, despite these advantages, the compression of water vapor presents substantial technical challenges. The low density of steam and the steep slope of its saturation curve require multiple compressor stages with intercooling, leading to increased system complexity and cost [1]. For example, Kriese et al. [3] demonstrated a water-based HTHP capable of reaching 200 °C at the heat sink using three turbocompressor stages and intermediate cooling, achieving a total temperature lift of 100 °C. Such requirements currently limit the widespread application of water-based HTHPs in industry and motivate the search for efficient alternatives to purely mechanical

Turbo Expo: Turbomachinery Technical Conference & Exposition (GT2026), June 15–19, 2026. GT2026.
[1]Corresponding author.
Manuscript received May 5, 2026; final manuscript received May 7, 2026; published online September 10, 2026. Editor: Jerzy T. Sawicki.

Copyright © 2026 by ASME; reuse license CC-BY 4.0

Downloaded from asmedigitalcollection.asme.org/gasturbinespower/article-pdf/148/12/121012/7632183/gtp-26-1257.pdf by Deutsches Zentrum für Luft- und Raumfahrt (DLR) user on 28 September 2026

steam compression. A promising solution to overcome the limitations of multistage steam compression is the integration of ejectors into HTHPs. Ejectors are passive fluid devices that utilize the momentum of a high-pressure motive fluid to entrain and compress a lower-pressure suction fluid. Their advantages include simplicity, absence of moving parts, and cost-effectiveness [4]. When properly designed, ejectors can mix high-pressure liquid water with superheated steam, achieving a simultaneous pressure lift and temperature reduction through the exchange of mass, momentum, and energy [5]. The ejector can reduce the mechanical compressor load by performing a portion of the compression process minimizing by that the number of required compressor stages and can eventually improve overall heat pump cycle efficiency. Previous numerical analyses by the authors [5–7] have shown that a water-based ejector integrated into an HTHP could increase the coefficient of performance by approximately 10%, achieving a pressure ratio of around 1.3, roughly 50–60% of what is typically achieved by turbocompressors.

Ejectors have been widely investigated in refrigeration and heat pump systems, particularly for working fluids such as CO_2, R290, and R600a. Elbel and Hrnjak [8] experimentally demonstrated efficiency improvements of up to 8% in a transcritical CO_2 ejector cycle compared to a conventional throttling system. Subsequent studies, including those by Banasiak et al. [9] and Lu et al. [10], systematically examined the influence of ejector geometry on two-phase performance. These investigations confirmed the strong sensitivity of entrainment ratio and pressure lift to both geometric parameters and operating conditions.

Relatively few studies, however, have focused on two-phase ejectors using water as the working fluid. Šarevski and Šarevski [11,12] investigated water ejectors in thermocompression-based refrigeration systems. Their initial work examined industrial concentrators employing thermocompression, where the ejector operated in conjunction with a water centrifugal compressor [11]. A subsequent configuration introduced mixing of compressor discharge vapor with high-pressure condensate inside a two-phase ejector [12]. While these studies demonstrated the general feasibility of water ejectors, the operating pressures and temperatures considered differ substantially from those relevant to HTHP applications. More recently, the authors demonstrated that integrating a two-phase ejector into a water-based HTHP can increase the coefficient of performance by approximately 9% and achieve a pressure ratio of about 1.3 [5].

Broader experimental investigations of water-driven ejectors have primarily addressed steam-based systems. Ma et al. [13] analyzed a solar-assisted steam ejector refrigerator and showed that ejector performance is strongly influenced by boiler temperature and spindle position. Zhang et al. [14] presented a water-driven steam injector for waste heat recovery and validated a one-dimensional two-fluid model capable of reproducing entrainment behavior and condensation-induced shock development. Their results indicated that higher steam inlet pressure and lower water temperature enhance entrainment, whereas back-pressure effects are comparatively weak. Additional experimental studies employing different working fluids further emphasized the complex interdependence between operating parameters and ejector performance. Wang and Yu [15] investigated a two-phase ejector using refrigerant R600a, while Shestopalov et al. [16] reported detailed experimental results for an ejector refrigeration machine operating with R245fa. Although these works provide valuable insight into ejector behavior, they rely on working fluids other than water and operate under conditions that are not representative of water-based HTHP applications. From an experimental facility perspective, ejector investigations have predominantly been conducted on laboratory-scale steam-jet refrigeration and thermocompression rigs, where the ejector is supplied by a boiler or steam generator and discharged against a controlled condenser or back-pressure level. Several studies describe such test rigs in detail and report operating maps, and in some cases include axial wall-pressure measurements to characterize mixing and pressure recovery within the ejector [17–19]. More recent work has highlighted the inherently two-phase nature of transonic steam ejector flows, employing optical access and high-speed visualization to resolve unsteady shock and condensation structures [20]. Complementary efforts have established experimental reference cases for steam ejectors that support Computational Fluid Dynamics (CFD) model validation, while simultaneously emphasizing the scarcity of well-instrumented datasets suitable for this purpose [21].

Although CFD and theoretical modeling have substantially improved the understanding of ejector behavior, experimental data for two-phase water ejectors under high-pressure motive fluid, high-temperature suction fluid conditions are nearly absent. The design, fabrication, and safe operation of a high-pressure, high-temperature water–steam ejector facility present considerable technical challenges, including precise control of inlet and outlet conditions, stable continuous operation, and accurate measurement under dynamic two-phase flow conditions. Without experimental validation, the applicability of CFD models and the reliability of design methods for such systems remain limited. As a result, there is a clear need for dedicated experimental infrastructure capable of generating reproducible and precisely controlled data under conditions relevant to industrial water HTHPs. The present work addresses this gap by introducing a novel high-pressure, high-temperature two-phase ejector test facility specifically designed for integration studies with water HTHPs. The facility enables continuous, closed-loop operation with flexible control of both water and steam conditions, covering motive pressures up to 125 bar and steam suction pressures up to 8 bar. It incorporates state-of-the-art measurement technologies, including high-accuracy static pressure sensors for wall pressure monitoring along the ejector axis, high-sensitivity piezoelectric sensors for detecting potential shock waves, vortex-type mass flow meters for flow measurement, and control valves that ensure continuous operation and stable back-pressure regulation throughout the system. The custom ejector design, developed from prior CFD optimization by the authors [7], features a fixed geometry optimized for controlled testing of operating parameters. The experimental facility developed for this work comprises a high-pressure piston pump, a large-capacity steam generator, and a configurable steam-conditioning unit that allows controlled adjustment of steam inlet states. The present paper introduces the mechanical and thermodynamic design of both the ejector and the associated test stand, outlines the measurement approach and instrumentation strategy, and reports preliminary observations from commissioning tests. These initial results serve as a proof of concept for evaluating the ejector as a secondary compression component in water-based HTHPs. The findings from this work are intended to support future modeling efforts and to facilitate improved integration of ejector technology into advanced water-based HTHP systems.

2 Ejector Working Principle

Figure 1 illustrates the operating concept of the two-phase water ejector investigated here. High-pressure liquid water enters the motive nozzle (1), where it undergoes rapid expansion and acceleration. The resulting high-velocity jet produces a region of reduced pressure at the nozzle exit, which induces the inflow of the suction fluid (B), superheated steam, through the suction nozzle (2) into the mixing chamber (3). As the two streams progress

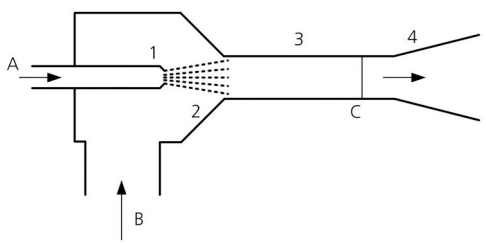


Fig. 1 General scheme of an ejector, description in text

Downloaded from asmedigitalcollection.asme.org/gasturbinespower/article-pdf/148/12/121012/7632183/gtp-26-1257.pdf by Deutsches Zentrum für Luft- und Raumfahrt (DLR) user on 28 September 2026

downstream, the liquid jet continues to expand while the entrained steam is accelerated, leading to an exchange of mass, momentum, and energy along the mixing section. Due to the back pressure imposed downstream of the ejector, a normal shock (C) typically develops after the mixing section, producing an abrupt increase in static pressure [22,23]. The speed of sound in the two-phase mixture is much lower than in either pure liquid water or vapor steam [24], allowing the mixture to reach supersonic conditions at comparatively modest velocities. This makes the formation of compression shocks possible, as will be discussed later in the results. Afterwards, the flow enters the diffuser (4), where it decelerates and gains additional static pressure. The overall performance of the ejector is commonly described using two nondimensional parameters, the pressure ratio and the entrainment ratio. The pressure ratio is defined as the ratio of the ejector outlet pressure to the suction fluid inlet pressure. The entrainment ratio is the ratio of the suction fluid mass flow rate to the motive fluid mass flow rate. Together, these parameters provide a concise characterization of the ejector's operating behavior and its influence on the efficiency of the heat-pump cycle.

3 Experimental Setup

In this section, the design and configuration of the experimental facility are presented. The description includes the overall layout of the test stand, the thermodynamic process, and the design of the two-phase ejector. Subsequently, the measurement and instrumentation systems are detailed, followed by the procedures for commissioning.

3.1 Overall Test Stand Design. Figure 2 illustrates the Process and Instrumentation Diagram (P&ID) of the ejector test facility. Steam generation is provided by the steam generator HP01, which delivers saturated steam at pressures of up to 12 bar and mass flow rates reaching 600 kg/h. Because stable, dry, and superheated steam is required at the ejector suction inlet, the steam undergoes several conditioning steps before entering the ejector. Upon leaving the steam generator, the steam is routed through a mud trap (HQB01) to remove solid impurities, followed by a cyclone separator (HPB01) that separates entrained condensate and directs it to the condensate line (WAP01). The conditioned steam then enters the steam conditioning section, which consists of two steam buffers (CM01 and CM02) arranged in series. These buffers serve to damp pressure fluctuations and provide thermal inertia, ensuring a stable steam supply to the ejector. Pressure control upstream of the buffers is achieved using two regulating valves. The first valve, RNB01, provides a coarse pressure reduction, while the second valve, RNB02, enables fine adjustment of the steam pressure. Superheating is achieved through controlled throttling across these valves. When saturated steam generated at elevated pressure in HP01 is expanded to the lower pressure required at the ejector suction inlet, the steam temperature remains approximately constant while the saturation temperature decreases, resulting in a defined degree of superheat. By selecting the generator pressure in HP01 and adjusting valves RNB01 and RNB02, the desired suction pressure and superheat level can be established.

Downstream of the buffers, the steam passes through a fine filter (HQB02) before entering the final control section. Two control valves, RNB03 and RNB06, are installed immediately upstream of the ejector suction nozzle. Valve RNB03 directs the conditioned steam to the ejector, while RNB06 allows excess steam to be diverted to the standpipe and vented to atmosphere. An integrated control strategy adjusts these valves to regulate both the suction pressure and mass flow rate. Pressure and temperature sensors are installed upstream and downstream of each control valve to continuously monitor the steam state. Condensate management is integrated throughout the steam line. Several steam traps (RNA01–RNA04) and associated drainage connections (WPA01–WPA04) remove condensate formed during operation and route it to the hall drainage system at the base of the standpipe. For overpressure protection, a safety valve (FLB01) set to 12 bara is installed upstream of the ejector suction line. On the motive side, pressurized liquid water is supplied by the high-pressure piston pump CPA01, which is capable of operating at pressures of up to 125 bar. Before entering the ejector, the water flows through a plate heat exchanger (EGC01), where it is heated to the required inlet temperature. The thermal energy for this process is recovered from the hot condensate discharged from the ejector, enabling partial internal heat recovery within the facility.

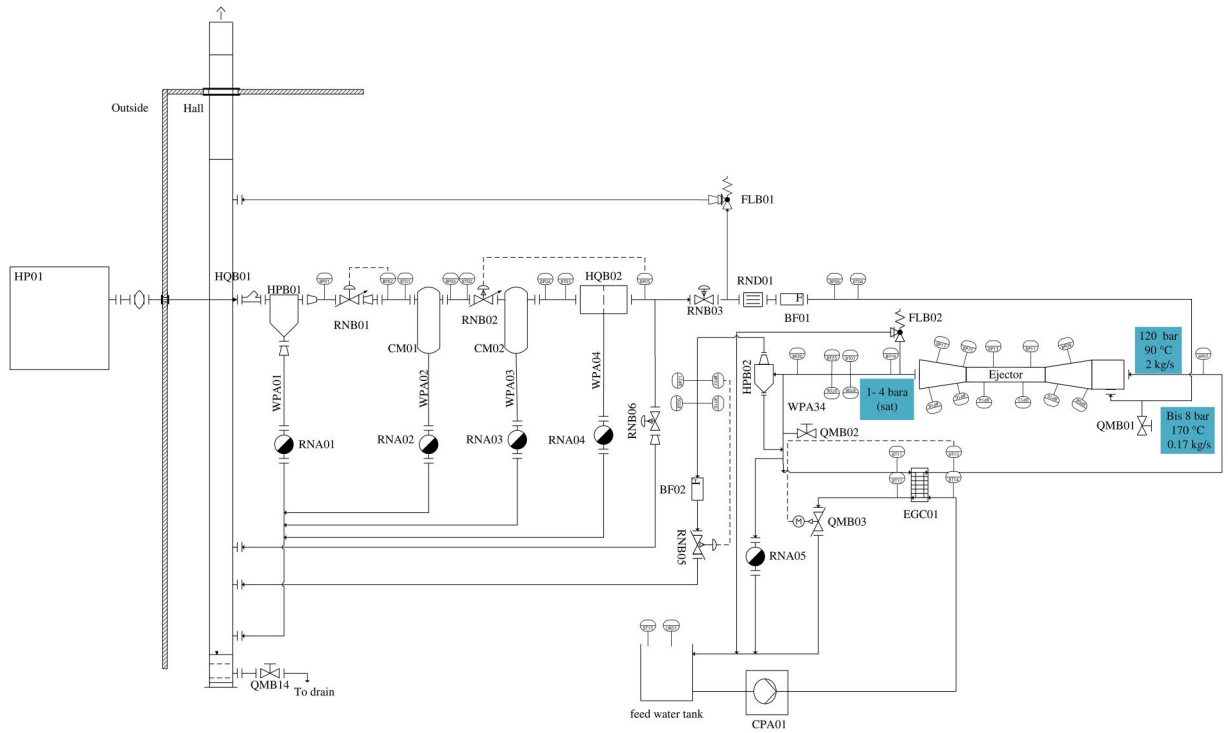


Fig. 2 P&ID of the ejector test stand; boxed values indicate the design limits of the test stand

Downloaded from asmedigitalcollection.asme.org/gasturbinespower/article-pdf/148/12/121012/7632183/gtp-26-1257.pdf by Deutsches Zentrum für Luft- und Raumfahrt (DLR) user on 28 September 2026



Fig. 3 Ejector test stand; the main components: 1, ejector; 2, inlet high-pressure water; 3, inlet-steam; 4, separator; 5, condensate line; 6, feed water tank; 7, water-piston pump; 8, back-pressure control valve; and 9, sight glass after the ejector outlet

Table 1 Key parameters of the ejector test stand

Parameter	Design/limit value
Motive (liquid water):	
Mass flow rate (max) (kg/s)	2
Inlet pressure (max) (bar)	125
Inlet temperature (max) (°C)	90
Suction (water vapor):	
Mass flow rate (max) (kg/s)	0.167
Inlet pressure (max) (bar)	8
Inlet temperature (max) (°C)	170
Outlet/operating range:	
Adjustable back pressure range (bar)	1–4
Expected pressure ratio range	1.0–1.5

As previously explained, inside the ejector, the high-pressure water expands through the motive nozzle, generating a high-velocity flow that entrains the superheated steam entering through the suction port. The resulting two-phase mixture forms in the mixing section, where mass, momentum, and energy exchange occur. The detailed design and geometry of the ejector are described later in Sec. 3.2. At the ejector outlet, the resulting two-phase mixture exits the ejector and enters the separator HPB02, where the liquid and vapor phases are separated. An auxiliary condensate branch (WPA34) installed upstream of the separator supports reliable removal of liquid water. At the base of this branch, control valve QMB03 directs approximately 70% of the condensate through the plate heat exchanger, while the remaining fraction is returned gradually to the feedwater tank via the condensate drain RNA05. The feedwater tank collects the returned condensate and supplies the high-pressure pump, thereby closing the water loop. On the vapor side, steam leaving the top of the separator passes through the back-pressure control valve RNB05. By adjusting this valve, the ejector outlet pressure can be precisely controlled, allowing systematic variation of operating conditions during experiments. To ensure piping safety, a safety valve (FLB02) is installed in the test stand. This valve protects the system by opening automatically if the pressure exceeds a predefined set point, thereby preventing potential pipe damage. Manual valves QMB01 and QMB02 are provided for condensate drainage when required. A photograph of the complete ejector test facility is shown in Fig. 3, with the principal components identified. The key operating parameters of the test stand are summarized in Table 1. The facility enables independent adjustment of motive and suction inlet conditions, as well as controlled regulation of the ejector outlet pressure.

3.2 Ejector Design. The ejector was designed to investigate the behavior of two-phase water–steam flows under high-pressure conditions relevant to high-temperature heat pumps. Its geometry was derived from prior CFD optimization studies conducted by the authors [7]. Figure 4 shows the two-dimensional drawing of the ejector, while Fig. 5 illustrates the corresponding three-dimensional technical model highlighting the main components; the motive nozzle (1), suction nozzle (2), mixing chamber (3), and diffuser (4).

The overall length of the ejector is approximately 1200 mm, and all components are fabricated from stainless steel to ensure compatibility with high-pressure water and the high-temperature steam. The motive nozzle is designed to accelerate the high-pressure liquid water to high velocity, generating a high-momentum fluid that entrains the incoming superheated steam from the suction port. To characterize these flow phenomena experimentally, 11 wall pressure ports were integrated along the axial direction of the ejector body. These ports enable local static pressure measurement needed to characterize the ejector performance and for comparison with CFD-predicted wall pressure distributions. Three of these ports in the critical region near the mixing-section exit and diffuser inlet are used

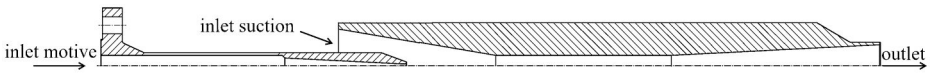


Fig. 4 Two-dimensional drawing of the upper half of the ejector (not to scale)

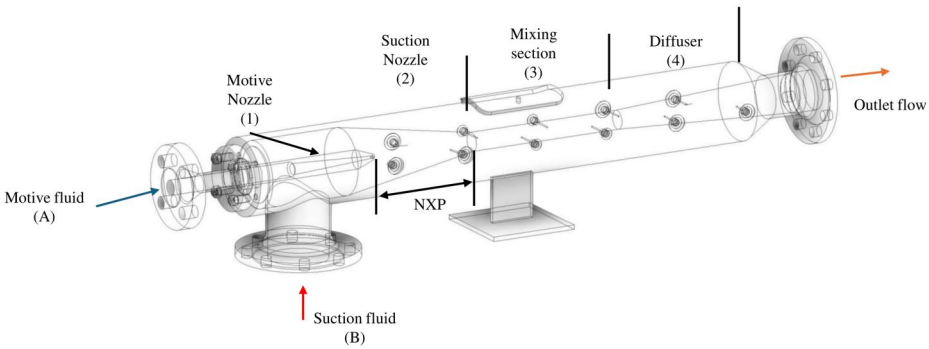


Fig. 5 Technical drawing of the ejector, manufactured by GEA Wiegand [25]

Downloaded from asmedigitalcollection.asme.org/gasturbinespower/article-pdf/148/12/121012/7632183/gtp-26-1257.pdf by Deutsches Zentrum für Luft- und Raumfahrt (DLR) user on 28 September 2026



Fig. 6 Ejector installed in test stand

for high-frequency dynamic pressure sensors. These sensors offer a high sampling rate, enabling the detection of very small pressure fluctuations and the identification of pressure waves associated with potential shock formation. Details of the installed sensor types, measurement principles, and data acquisition strategy are presented in Sec. 3.3. Figure 6 presents a photograph of the ejector mounted in the test stand.

Figure 7 shows representative CFD pressure and velocity contours of the ejector under study. The figures show the expansion of the motive fluid, the mixing between the two phases, and the formation of a normal shock wave at the end of the mixing section. For improved visualization, the static pressure contour is limited to a maximum value of 150 kPa and referenced relative to atmospheric pressure. As a result, the motive nozzle inlet lies outsidie the plotted range since its pressure of 120,000 kPa exeeds the range shwon in the figure. The pressure field reveals a progressive decrease along the mixing section, followed by distinct flow regions. A pronounced low-pressure zone forms near the end of the mixer, after which a normal shock raises the pressure to the specified diffuser outlet level. The velocity contour highlights the contraction of the jet core as the motive stream exits the nozzle and interacts with the suction flow, which is entrained into the jet. Within the mixing region, the velocity rises as momentum is transferred between the two streams. In the vicinity of the normal shock, high velocities are concentrated along the ejector's centerline.

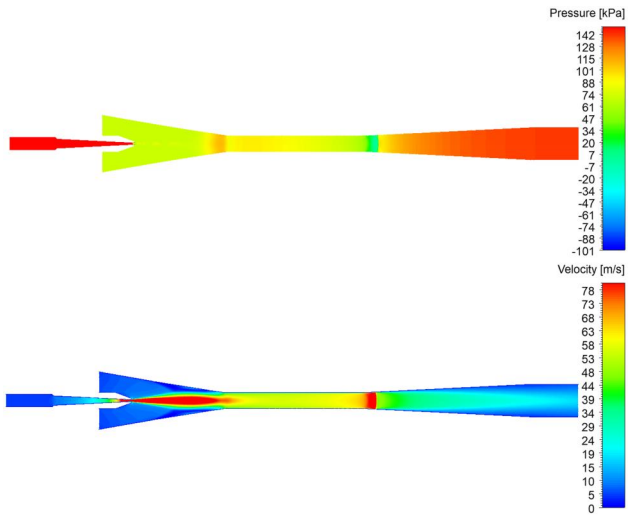


Fig. 7 Contours of gauge pressure (top) and velocity (bottom) along the ejector; inlet motive pressure: 120 bar, at 90 °C, inlet suction pressure: 1.7 bar, at 145 °C, and back-pressure is set at 2.09 bar at saturation condition, from Ref. [7]

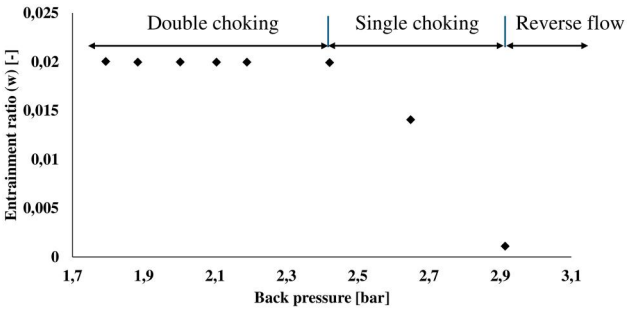


Fig. 8 Ejector performance curve obtained from CFD simulations

Figure 8 presents the CFD-predicted performance curve of the ejector, illustrating the variation of entrainment ratio with increasing back pressure. At low and moderate back-pressure levels, the entrainment ratio remains essentially constant, indicating double-choking conditions in which both the motive and suction streams are choked and the mass flow rates of both inlets have reached their maximum possible values. As the back pressure continues to rise, the system reaches a critical point, beyond which the entrainment ratio drops sharply. Past this point, the ejector transitions into the single-choking regime, where only the motive flow remains choked while the suction flow becomes unchoked and progressively suppressed by the increasing downstream pressure. This regime is typically narrow, and further increases in back pressure eventually lead to breakdown of ejector operation, characterized by zero entrainment and backflow.

3.3 Measurement System. The measurement and data acquisition system was designed to capture both steady-state and transient flow phenomena occurring in the ejector test stand. The locations of all sensors are shown in the P&ID in Fig. 2. A combination of static and high-frequency pressure sensors, together with temperature and mass flow measurements, is employed to monitor the operating conditions and the internal flow behavior within the ejector.

To characterize the pressure distribution and dynamic response within the ejector, three types of pressure sensors were installed. Keller Series 23SX piezoresistive pressure sensors were used to record static pressures. They are placed after the ejector outlet and separator. The downstream sensors are used for feedback control of the back-pressure valve (RNB05). Placement directly at the ejector exit was avoided to prevent reading fluctuations caused by high-velocity two-phase flow (up to 35–40 m/s as shown in Fig. 7).

Along the ejector body, eight PTA225 EFE high-accuracy piezoresistive pressure sensors are installed on the holes drilled on the ejector body to measure wall static pressures. These sensors offer

Downloaded from asmedigitalcollection.asme.org/gasturbinespower/article-pdf/148/12/121012/7632183/gtp-26-1257.pdf by Deutsches Zentrum für Luft- und Raumfahrt (DLR) user on 28 September 2026

an accuracy of ±0.05% of full scale and a sampling frequency up to 1 kHz, making them suitable for monitoring both steady and moderate dynamic pressure variations. Three PCB 112B05 piezoelectric dynamic pressure sensors are positioned at the transition between the mixing chamber and the diffuser, a region where shock waves are expected to occur. These sensors provide a frequency response above 250 kHz and are designed to resolve high-speed transient phenomena, including shock formation, propagation, and very small pressure fluctuations. Each sensor is equipped with an inline charge amplifier and dedicated power supply unit, ensuring signal fidelity. These measurements will be used in future work to perform frequency-domain analyses (FFT) and to validate transient pressure fluctuations predicted by CFD simulations.

Two types of sensors are employed for temperature measurement. KROHNE OPTITEMP TRA-S 11 resistance temperatures detectors (Pt100) thermometers are placed on the inlet and outlet of the plate heat exchanger, and the downstream sensor on the high-pressure water side is used to regulate the condensate valve (QMB03). All remaining temperature measurements are taken using sheathed Type-K thermocouples equipped with thermocouple connectors.

The mass flow rates of the motive and suction flows are determined using two separate measurement approaches. The motive water mass flow is derived from the pump control system, which calculates the flow rate based on the measured rotational speed in combination with the pump's characteristic curve. For the suction stream, the incoming steam mass flow is measured upstream of the ejector using a KROHNE OPTISWIRL 4200 C vortex flowmeter. Downstream of the ejector, the flow leaving the separator is assumed to be in a single-phase state. The vapor discharged from the separator is likewise monitored with a KROHNE OPTISWIRL 4200 C vortex flowmeter, allowing accurate determination of the vapor mass flow rate at the separator outlet. The comparison between the suction-line and separator-outlet mass flow rates provides critical information on the thermodynamic processes occurring inside the ejector, including condensation and evaporation phenomena. In particular, deviations between the two measurements can indicate the extent of steam condensation induced by the mixing process or by the pressure-increase shock, as well as potential flashing or evaporation of the motive fluid within the ejector body. All sensors and valves are connected to a Siemens S7 Programable Logic Controller that handles data acquisition and system control.

4 Commissioning and Initial Results

This section outlines the procedures and preliminary observations from the commissioning phase of the ejector test facility. The commissioning activities aimed to verify mechanical integrity, confirm proper operation of the instrumentation, and assess the functionality of the motive nozzle and ejector assembly under single-phase water conditions and two-phase water-steam operation.

4.1 Motive Nozzle Spray Tests. The motive nozzle used in this study was custom-designed and manufactured to withstand the high-pressure and high-temperature operating conditions of the motive flow (max 120 bar and 90 °C as shown in Table 1). Due to these specialized requirements, no manufacturer data were available regarding its external spray characteristics or discharge behavior. Figure 9 presents the technical drawing of the motive nozzle.

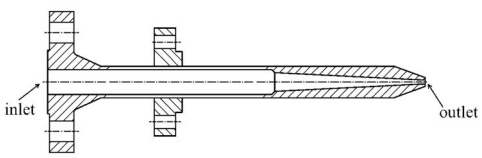


Fig. 9 Technical drawing of the motive nozzle (not to scale)



Fig. 10 Open-air motive nozzle test showing the spray pattern at 120 bar and ambient temperature

To obtain an initial qualitative understanding of the jet behavior, the nozzle was tested independently outside the ejector under ambient conditions. High-pressure water at approximately 120 bar was discharged freely into the air, with the water temperature near 15 °C. Figure 10 shows a frame captured during the open-air test, revealing the spray pattern emerging from the nozzle exit. The flow appears initially compact and axisymmetric, forming a nearly flat jet core that gradually diverges downstream. After roughly 0.5 m, the jet transitions into a highly turbulent and finely dispersed on the spray sides with the core of the jet remaining flat. This behavior is indicative of atomization effects caused by the high injection pressure and liquid velocity, which are subjected to strong shear forces exerted by the surrounding static air. These observations are consistent with the characteristics of atomized high-pressure water jets reported in the literature [26]. Trettel [26] evaluated the jet breakup regime for high-pressure liquid jets and introduced three characteristic dimensionless numbers, i.e., the Ohnesorge number, Weber number, and Reynolds number which together determine the breakup regime of a water exiting a nozzle. These are defined respectively as

$$\mathrm{Oh}_{\ell 0} \equiv \frac{\mu_\ell}{\sqrt{\rho_\ell \, \sigma \, d_0}} \tag{1}$$

$$\mathrm{We}_{\ell 0} \equiv \frac{\rho_\ell \, \bar{U}_0^2 \, d_0}{\sigma} \tag{2}$$

$$\mathrm{Re}_{\ell 0} \equiv \frac{\bar{U}_0 \, d_0}{\nu_\ell} \tag{3}$$

where μ_ℓ is the liquid dynamic viscosity, ρ_ℓ is the liquid density, σ is the liquid surface tension, d_0 is the nozzle exit diameter, $\bar{U}_0$ is the mean jet exit velocity, and ν_ℓ is the liquid kinematic viscosity. The Ohnesorge number quantifies the relative importance of viscous forces compared to inertial and surface tension forces, the Weber number represents the ratio of inertial to surface tension forces, and the Reynolds number characterizes the ratio of inertial to viscous forces. Under the operating conditions of the nozzle tests, all three characteristic numbers reach values characteristic of atomizing liquid jets, indicating that the flow resides in the atomization region. This test was necessary to determine whether the high-pressure water jet would become finely dispersed and atomized inside the ejector, as this behavior strongly influences how the liquid interacts with the superheated steam entering through the suction line.

Following the completion of the test stand construction, a tightness and sensor verification test was conducted to ensure correct operation of the measurement system and mechanical integrity of the piping under high-pressure conditions. During this test, the motive nozzle was re-installed in the ejector body and supplied with pressurized liquid water at 120 bar. The suction, back-pressure, and condensate lines were fully open to the atmosphere, corresponding to operation without applied back pressure. This procedure allowed verification of the sensors signals, test stand tightness, and qualitative visualization of the internal flow.

A transparent sight glass positioned approximately 1 m downstream of the ejector outlet (see component 9 in Fig. 3) provided direct visual access to the flow inside the pipe after the ejector. Figure 11 shows a frame captured during the tightness test. From the

Downloaded from asmedigitalcollection.asme.org/gasturbinespower/article-pdf/148/12/121012/7632183/gtp-26-1257.pdf by Deutsches Zentrum für Luft- und Raumfahrt (DLR) user on 28 September 2026



Fig. 11 Flow visualization through sight glass during water-only operation

figure, it can be seen that the observed flow pattern differed markedly from the open-air test: rather than a coherent jet core, the flow exhibited strong turbulence and rapid mixing within the pipe. This behavior may be attributed to the geometric confinement of the ejector mixing section and the downstream piping as previously presented in Fig. 4. According to CFD results (Fig. 7), the velocity at the motive nozzle exit reaches approximately 150 m/s. Combined with the no-slip boundary condition at the wall, this generates steep velocity gradients and shear-induced turbulence, consistent with the experimentally observed flow behavior in the sight glass.

4.2 Test Stand Start-Up Procedure. The commissioning of the test stand follows a defined start-up sequence to ensure safe thermal conditioning of the facility and stable operation. The procedure begins by activating the steam generator and introducing steam at approximately 1 bar throughout the system while all valves remain fully open. This initial flushing step gradually warms the piping network and instrumentation without imposing back pressure.

Since the steam generator supplies saturated steam at pressures up to 8 bar, the required degree of superheat is generated in the downstream steam-conditioning unit. Here, a series of control valves throttle the steam to the desired operating pressure, leading to a temperature rise above saturation. Through a combination of throttling stages and bypass lines, the steam pressure, superheat level, and mass flow rate can be adjusted.

Once the piping and components are thermally stabilized, the back-pressure valve is gradually closed until the target back-pressure at the ejector outlet is reached. At this stage, only the steam loop is active. When the steam circuit reaches steady conditions, the high-pressure water pump is started and water is supplied to the motive nozzle at moderate pressures (10 to 60 bar increased in steps). During this phase, the superheated steam provides the thermal energy needed to preheat the water. Owing to the high heat capacity of liquid water, only a small steam flow is required to raise the water temperature. Heating continues until the temperature measured downstream of the plate heat exchanger on the high-pressure water side reaches approximately 60 °C. Thereafter, the motive-flow pressure is increased in controlled increments until the desired operating conditions are achieved.

4.3 Initial Results. Figure 12 illustrates a snapshot of the test stand control interface, presenting the real-time operating conditions for four distinct operating points. The high-pressure piston pump supplied liquid water at motive pressures of 90, 100, 110, and 120 bar. The pressurized water was first routed through a plate heat exchanger, where its temperature increased prior to entering the motive nozzle. With increasing motive pressure, the water mass flow rate also increased, in accordance with the pump characteristics. This resulted in enhanced heat transfer within the plate heat exchanger and, consequently, a higher motive water temperature at the nozzle inlet. On the suction side, superheated steam was supplied under approximately constant operating conditions, with a mass flow rate of about 450 kg/h, a temperature of roughly 135 °C, and a pressure of 1.91 bar. During all measurements, the back-pressure control valve downstream of the ejector was kept at a fixed opening position of 3%. This parameter study was conducted to assess the influence of the motive water pressure on the ejector performance. Figure 13 presents the resulting pressure ratio and entrainment ratio as functions of the motive fluid inlet pressure. The results indicate

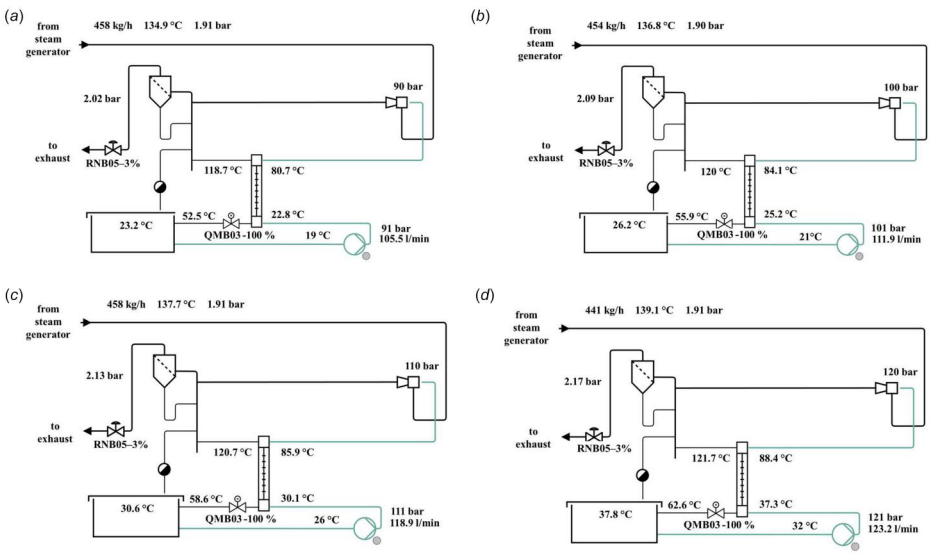


Fig. 12 Control interface visualization of the ejector test stand showing real-time operating conditions at four motive water pressure levels: (*a*) 90 bar, (*b*) 100 bar, (*c*) 110 bar, and (*d*) 120 bar. Displayed parameters include the motive and suction fluids inlet conditions, and the back pressure downstream of the separator.

Downloaded from asmedigitalcollection.asme.org/gasturbinespower/article-pdf/148/12/121012/7632183/gtp-26-1257.pdf by Deutsches Zentrum für Luft- und Raumfahrt (DLR) user on 28 September 2026

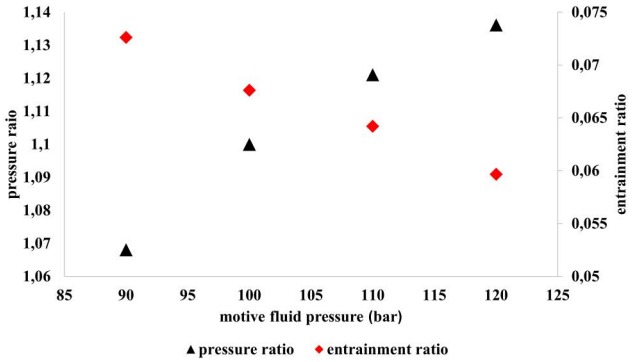


Fig. 13 Ejector pressure ratio and entrainment ratio as functions of the motive water inlet pressure, based on the four operating points shown in Fig. 12

that increasing the motive pressure leads to a higher pressure ratio, while the entrainment ratio decreases.

This behavior can be attributed to the increased momentum transfer associated with higher motive pressures, which intensifies the compression process and strengthens shock structures within the ejector. At the same time, since the suction steam conditions were held almost constant, the rise in motive pressure was accompanied by an increase in the motive water mass flow rate, thereby reducing the entrainment ratio. Under the investigated operating conditions, the ejector achieved a maximum pressure ratio of approximately 1.15 at an entrainment ratio of about 0.06.

Figure 14 shows the pressure ratio and entrainment ratio as functions of the suction fluid inlet pressure. Three suction pressure levels were investigated while maintaining constant motive side operating conditions, namely, a motive water pressure of 120 bar, a volumetric flow rate of 123 L/min, and a motive water inlet temperature of approximately 90 °C. The back-pressure valve opening was also kept here at an opening of 3%. The results indicate that an increase in suction fluid inlet pressure leads to a higher entrainment ratio and a lower pressure ratio. This behavior may be attributed to the higher suction pressure causing the induction of a larger steam mass flow into the ejector mixing section. At the same time, the reduced pressure difference between the suction inlet and the ejector outlet limits the achievable pressure rise, thereby lowering the pressure ratio.

As previously said, several observations and challenges in operation occurred during these initial runs. First, the suction effect of the ejector was considerably stronger than simulated. Although the steam inlet conditions were predetermined in the steam-conditioning unit, the injection of high-pressure water flow in the ejector's motive nozzle caused a noticeable reduction of the suction-line steam pressure, on the order of 0.4 bar, and an associated increase in the sucked steam mass flow rate.

Second, the water temperature in the feed tank rose rapidly during operation. The high-pressure pump has a safety feature that shuts down automatically when its inlet temperature exceeds 40 °C. Therefore, several tests were interrupted prematurely. To enable continuous operation, an external cooling loop will be added to regulate the water-tank temperature.

Third, the back-pressure valve RNB05 was found to be oversized for the current operating range. During the tests, the valve operated almost completely closed (the valve opening position remained in the 2–5% range throughout the experiments), limiting the ability to investigate a wider range of back-pressure values at the ejector outlet. This valve will be replaced with a smaller, more suitable unit in the next measurement campaign.

Additionally, upcoming experiments will include detailed analysis of the pressure distribution along the ejector wall and mass-flow measurements downstream of the separator on the steam side. In addition, a systematic parameter study will be carried out to investigate a range of motive and suction operating conditions. The resulting dataset will provide a basis for validating numerical simulations and for improving the understanding of two-phase flow behavior inside the ejector body.

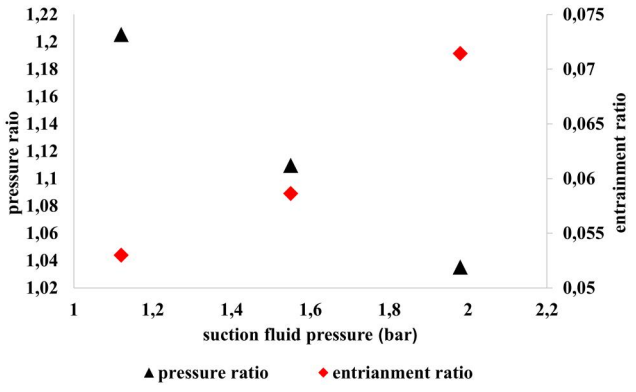


Fig. 14 Ejector pressure ratio and entrainment ratio as functions of the suction fluid inlet pressure

5 Conclusion

This work has presented the design and realization of a novel two-phase water ejector together with a large-scale closed-loop experimental facility developed specifically for evaluating ejectors as secondary compression components in high-temperature water heat pumps. The paper detailed the mechanical design of the ejector, the configuration of the test stand, and the measurement architecture required to operate the system safely and accurately under high-pressure and high-temperature conditions.

The initial commissioning results demonstrate that the ejector can achieve pressure ratios of up to approximately 1.15 and entrainment ratios of about 0.06 under the preliminary operating conditions tested. These preliminary results demonstrate that two-phase water ejectors can operate as effective secondary compression stages in water-based high-temperature heat pumps, highlighting their potential as nonmechanical auxiliary compression devices.

Future work will focus on refining the operational stability of the test stand particularly with respect to thermal management and back-pressure regulation and on expanding the experimental campaign. A systematic parametric study will be conducted to map the ejector performance across a broader range of operating conditions, accompanied by detailed wall-pressure measurements and vapor-quality analysis at the ejector outlet. These advancements will enable comprehensive validation of numerical models and deepen the understanding of two-phase flow dynamics in high-pressure ejectors.

Acknowledgment

The authors would like to thank the team at the German Aerospace Center (DLR) in Zittau for their technical and administrative support throughout the development of the experimental facility. The authors also gratefully acknowledge the use of the DLR high-performance computing infrastructures CARA and CARO, which enabled the large-scale simulations supporting the ejector design presented in this work.

Conflict of Interest

There are no conflicts of interest.

Data Availability Statement

The datasets generated and supporting the findings of this article are obtainable from the corresponding author upon reasonable request.

Downloaded from asmedigitalcollection.asme.org/gasturbinespower/article-pdf/148/12/121012/7632183/gtp-26-1257.pdf by Deutsches Zentrum für Luft- und Raumfahrt (DLR) user on 28 September 2026

References

[1] Arpagaus, C., Bless, F., Uhlmann, M., Schiffmann, J., and Bertsch, S. S., 2018, "High Temperature Heat Pumps: Market Overview, State of the Art, Research Status, Refrigerants, and Application Potentials," Energy, **152**, pp. 985–1010.

[2] Zühlsdorf, B., Schlemminger, C., Bantle, M., Evenmo, K., and Elmegaard, B., 2018, "Design Recommendations for R-718 Heat Pumps in High Temperature Applications," 13th IIR Gustav Lorentzen Conference, Valencia, Spain, June 18–20, pp. 1–10.

[3] Kriese, M., Klöppel, S., Setzepfand, N., Schaffrath, R., and Nicke, E., 2023, "Part-Load Behavior and Start Up Procedure of a Reverse Rankine High Temperature Heat Pump With Water As Its Working Medium," ASME Paper No. GT2023-103410.

[4] Besagni, G., Mereu, R., and Inzoli, F., 2016, "Ejector Refrigeration: A Comprehensive Review," Renewable Sustainable Energy Rev., **53**, pp. 373–407.

[5] Abu Khass, O., Tran, A. P., Klöppel, S., and Stathopoulos, P., 2023, "Modelling of Two-Phase Water Ejector in Rankine Cycle High Temperature Heat Pumps," ASME Paper No. GT2023-101245.

[6] Abu Khass, O., Tran, A. P., Klöppel, S., Stathopoulos, P., and Nicke, E., 2024, "1D Modelling of a Water-Steam Ejector as a Compression Step in High-Temperature Heat Pumps," ASME Paper No. GT2024-124983.

[7] Abu Khass, O., Cristofaro, M., Kopparthy, S. B., Klöppel, S., Nicke, E., and Stathopoulos, P., 2025, "Numerical Investigation of Two-Phase Water Ejectors for High-Temperature Heat Pumps: Insights Into Flow Behavior and Shock Wave Dynamics," ASME Paper No. GT2025-151706.

[8] Elbel, S., and Hrnjak, P., 2008, "Ejector Refrigeration: An Overview of Historical and Present Developments With an Emphasis on Air-Conditioning Applications," International Refrigeration and Air Conditioning Conference, West Lafayette, IN, July 14–17, Paper No. 884.

[9] Banasiak, K., Hafner, A., and Andresen, T., 2012, "Experimental and Numerical Investigation of the Influence of the Two-Phase Ejector Geometry on the Performance of the R744 Heat Pump," Int. J. Refrig., **35**(6), pp. 1617–1625.

[10] Lu, Y., Bai, T., and Yu, J., 2023, "Investigation on the Influence of Geometric Parameters on Two-Phase Ejector Performance With R290," Int. J. Refrig., **156**, pp. 102–112.

[11] Šarevski, M. N., and Šarevski, V. N., 2014, "Preliminary Study of a Novel R718 Refrigeration Cycle With Single Stage Centrifugal Compressor and Two-Phase Ejector," Int. J. Refrig., **40**, pp. 435–449.

[12] Šarevski, V., and Šarevski, M., 2012, "Energy Efficiency of the Thermocompression Refrigerating and Heat Pump Systems," Int. J. Refrig., **35**(4), pp. 1067–1079.

[13] Ma, X., Zhang, W., Omer, S., and Riffat, S., 2010, "Experimental Investigation of a Novel Steam Ejector Refrigerator Suitable for Solar Energy Applications," Appl. Therm. Eng., **30**(11–12), pp. 1320–1325.

[14] Zhang, Z., Chong, D., and Yan, J., 2012, "Modeling and Experimental Investigation on Water-Driven Steam Injector for Waste Heat Recovery," Appl. Therm. Eng., **40**, pp. 189–197.

[15] Wang, X., and Yu, J., 2016, "Experimental Investigation on Two-Phase Driven Ejector Performance in a Novel Ejector Enhanced Refrigeration System," Energy Convers. Manage., **111**, pp. 391–400.

[16] Shestopalov, K., Huang, B., Petrenko, V., and Volovyk, O., 2015, "Investigation of an Experimental Ejector Refrigeration Machine Operating With Refrigerant R245fa at Design and Off-Design Working Conditions. Part 2. Theoretical and Experimental Results," Int. J. Refrig., **55**, pp. 212–223.

[17] Chunnanond, K., and Aphornratana, S., 2004, "An Experimental Investigation of a Steam Ejector Refrigerator: The Analysis of the Pressure Profile Along the Ejector," Appl. Therm. Eng., **24**(2–3), pp. 311–322.

[18] Varga, S., Oliveira, A. C., Ma, X., Omer, S. A., Zhang, W., and Riffat, S. B., 2011, "Experimental and Numerical Analysis of a Variable Area Ratio Steam Ejector," Int. J. Refrig., **34**(7), pp. 1668–1675.

[19] Chandra, V. V., and Ahmed, M., 2014, "Experimental and Computational Studies on a Steam Jet Refrigeration System With Constant Area and Variable Area Ejectors," Energy Convers. Manage., **79**, pp. 377–386.

[20] Tang, Y., Liu, Z., Li, Y., Wu, H., Zhang, X., and Yang, N., 2019, "Visualization Experimental Study of the Condensing Flow Regime in the Transonic Mixing Process of Desalination-Oriented Steam Ejector," Energy Convers. Manage., **197**, p. 111849.

[21] Mazzelli, F., Giacomelli, F., and Milazzo, A., 2018, "CFD Modeling of Condensing Steam Ejectors: Comparison With an Experimental Test-Case," Int. J. Therm. Sci., **127**, pp. 7–18.

[22] Huang, B., Chang, J., Wang, C., and Petrenko, V., 1999, "A 1-D Analysis of Ejector Performance," Int. J. Refrig., **22**(5), pp. 354–364.

[23] Grazzini, G., Milazzo, A., and Mazzelli, F., 2018, *Ejectors for Efficient Refrigeration: Design, Applications and Computational Fluid Dynamics*, Springer, Cham, Switzerland.

[24] De Lorenzo, M., Lafon, P., Seynhaeve, J.-M., and Bartosiewicz, Y., 2017, "Benchmark of Delayed Equilibrium Model (DEM) and Classic Two-Phase Critical Flow Models Against Experimental Data," Int. J. Multiphase Flow, **92**, pp. 112–130.

[25] GEA Group, 2024, "Ejector Systems," GEA Wiegand GmbH, Ettlingen, Germany, accessed Nov. 9, 2024, https://www.gea.com/de/careers/school-students/ettlingen/

[26] Trettel, B., 2020, "Reevaluating the Jet Breakup Regime Diagram," Atomization Sprays, **30**(7), pp. 517–556.

Downloaded from asmedigitalcollection.asme.org/gasturbinespower/article-pdf/148/12/121012/7632183/gtp-26-1257.pdf by Deutsches Zentrum für Luft- und Raumfahrt (DLR) user on 28 September 2026